ACS APPLIED MATERIALS & INTERFACES

Research Article

www.acsami.org

Carbon Nanotubes Enhanced Fluorinated Polyurethane Macroporous Membranes for Waterproof and Breathable Application

Yang Li,[†,§] Zhigao Zhu,[†,§] Jianyong Yu,[‡,§] and Bin Ding*[,†,‡,§]

[†]State Key Laboratory for Modification of Chemical Fibers and Polymer Materials, College of Material Science and Engineering, Donghua University, Shanghai 201620, China

[‡]Key Laboratory of Textile Science & Technology, Ministry of Education, College of Textiles, Donghua University, Shanghai 201620, China

[§]Nanomaterials Research Center, Modern Textile Institute, Donghua University, Shanghai 200051, China

Supporting Information

ABSTRACT: Waterproof and breathable macroporous membranes that are both completely resistant to liquid water penetration and easily allowable to vapor transmission would have significant implication for numerous applications; however, fabrication of such materials has proven to be tremendously challenging. Herein, we reported novel electrospun composite fibrous membranes with high waterproof and breathable performance, which consisted of polyurethane (PU), terminal fluorinated polyurethane (FPU), and carbon nanotubes (CNTs). Benefiting from the utilization of FPU and CNTs, the fibrous membranes were endowed with superhydrophobic surface, optimized pores size and porosity, along with enhanced fibers, which resulted in excellent waterproof, breathable and mechanical properties. Significantly, the relationship among waterproofness, pore structure and surface wettability has been confirmed finely accordance with Young−Laplace equation. Ultimately, the resultant membranes presented high waterproofness with hydrostatic pressure up to 108 kPa, good breathability with water vapor transmission rate over 9.2 kg m^{-2} d^{-1}, as well as robust mechanical properties with bursting strength of 47.6 kPa and tensile strength of 12.5 MPa, suggesting them as promising alternatives for a number of potential applications, such as protective clothing.

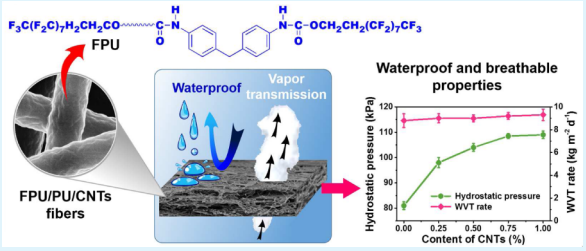

KEYWORDS: *electrospinning, terminal fluorinated polyurethane, carbon nanotubes, macroporous membrane, waterproof and breathable*

1. INTRODUCTION

Macroporous membranes that could strictly resist the penetration of liquid water while easily transmitting water vapor molecules have brought a revolution in a number of practical applications, including protective clothing and shoes, filter and separator media, and medical supplies.[1−4] In general, the fascinating properties of resistance to water droplets penetration and the admittance to water vapor and gases transmission of these membranes are generated from the utilization of hydrophobic raw materials, which turns the porous structure into interconnected passageway with hydrophobic walls.[5,6] Accordingly, the waterproof and breathable performance could be improved not only by minimization of pore size to withstand water penetration, but also maximization of porosity to transmit more water vapor.[7,8]

Up to now, various conventional techniques have been employed to fabricate macroporous membranes with waterproofness and breathability, including mechanical fibrillation,[9] template methods,[10] and melt blown.[11] Nevertheless, these methods are considered to be complicated in controlling, time-consuming, and high cost, as well as inappropriate in regulating pore size and porosity, to meet the requirement of better waterproof and breathable performance.

Recently, electrospinning has proved to be an alternative to these methods, which could facilely fabricate macroporous membranes by accumulating of fibers, moreover, the porous structure could be controlled simply by regulating fiber diameter and packing density.[12−14] Owing to these advantageous features, a lot of research efforts have been made to fabricate waterproof and breathable macroporous membranes. In 2007, polyurethane (PU) was first used to prepare waterproof and breathable fibrous membranes with macroporous structure, which exhibited limited waterproofness with hydrostatic pressure of 3.7 kPa but good breathability with water vapor transmission (WVT) rate of 9 kg m^{-2} d^{-1}.[15] Further investigation had been done by utilizing thinner fibers, which resulted in higher hydrostatic pressure of 80 kPa but depressed WVT rate of 4.3 kg m^{-2} d^{-1}.[16] In our previous study,

Received: April 1, 2015
Accepted: June 3, 2015
Published: June 3, 2015

DOI: 10.1021/acsami.5b02848
ACS Appl. Mater. Interfaces 2015, 7, 13538−13546

we reported a strategy for fabricating electrospun fibrous membranes with waterproof and breathable properties by introducing low surface energy materials, which exhibited medium hydrostatic pressure of 39.3 kPa along with high WVT rate of 9.2 kg m^{-2} d^{-1}.[17] Also reported in our recent study is that by modifying polyacrylonitrile fibrous membranes with waterborne polyurethane (WFPU) emulsion, we obtained waterproof and breathable fibrous membranes with hydrostatic pressure of 83.4 kPa and WVT rate of 9.2 kg m^{-2} d^{-1}; however, this strategy suffered from the complicated modification procedure with WFPU emulsion.[18] Therefore, to satisfy the requirement of practical application, waterproof, and breathable fibrous membranes with improved performance and easy fabrication method are still in urgent demand.

Intending to obtain electrospun fibrous membranes with better waterproof and breathable performance, the fibrous membranes should be promoted by other stimulative additive, besides the low surface energy component. Carbon nanotubes (CNTs) has been used as a promising nanofiller to prepare electrospun composite fibers and fibrous membranes because of the extraordinary ability to improve mechanical, antifouling, and electrical properties,[19] as well as obtainment of uniform fibers and pores,[20] which could result in improvement of waterproof and breathable performance of eleetrospun fibrous membranes.

On the other hand, the resistance of water penetration of macroporous membranes has already known to be related to the capillary force which is generated from hydrophobic feature and small pore size of the porous structure.[21,22] However, the electrospun macroporous membranes are constructed via accumulating of fibers during electrospinning process, which result in torturous interconnected porous structures and complex situation for liquid water flow through the membranes.[23,24] Therefore, accurate investigation of the dependence of waterproof and breathable properties on the intrinsic structure characteristic is significant and complicated, scarce efforts have focus on this problem.

In this study, we have designed and fabricated a kind of composite fibrous membranes with waterproof and breathable performance via electrospinning. The composite fibrous membranes consist of PU as substrate polymer, terminal fluorinated polyurethane (FPU) as low surface energy content, and CNTs as inspiring additive. Significantly, waterproof, breathable, and mechanical properties of the fibrous membranes were thoroughly investigated basing on surface wettability, fiber construction, and porous structure, which were regulated be tuning the concentrations of polymers solutions and the contents of CNTs. Furthermore, Young–Laplace equation was employed to estimate the dependence of hydrostatic pressure on the pore structure and surface wettability. Ultimately, FPU/PU/CNTs fibrous membranes with superhydrophobic surface, optimized porous structure and reinforced fibers were obtained, which exhibited robust waterproof, breathable, and mechanical performance.

2. EXPERIMENTAL SECTION

2.1. Materials. PU (Elastollan 2280A10, M_w = 180 000 g mol^{-1}, density = 1.13 g cm^{-3}) was purchased from BASF Polyurethane Specialties Co., Ltd., China. Multiwall carbon nanotubes (CNTs, average diameter = 8 nm, length = 1–30 μm, purity > 95 wt %) were bought from Chengdu Organic Chemicals Co., Ltd., China. Perfluoro-1-decanol ($CF_3(CF_2)_7CH_2CH_2OH$, TEOH-8) was obtained from Hengtong Fluorine CO., Ltd., China. 4.4′-Methylenebisphenylisocyanate (MDI), polytetramethylene ether glycol (PTMEG, M_n = 1000 g mol^{-1}), triethylene glycol (TEG), *N*,*N*-dimethylformamide (DMF), dimethylacetamide (DMAc), tetrahydrofuran (THF), anhydrous calcium chloride ($CaCl_2$), and methanol were provided by Aladdin Chemical Reagent Co., Ltd., China. All chemicals were of analytical grade and were used as received without further purification.

2.2. Synthesis of Terminal Fluorinated Polyurethane. The FPU was synthesized according to a three-step polymerization route (as shown in Figure S1, Supporting Information) described in our previous works.[25] Typically, a mixture of TEOH-8 (9.28 g) and DMF (8 g) was added dropwise into a flask containing 12.5 g of MDI and 12 g of DMF. After the mixture was stirred at 50 °C for 2 h, PTMEG (7.5 g) was added slowly to the above solution as soft segment to give a chain extending reaction at 60 °C for 2 h. Subsequently, TEG (2 g) as a chain extender was poured into the flask and stirred at 70 °C for 2 h, then the mixture was heated to 80 °C, followed by the addition of 2.32 g of TEOH-8 and 2 g of DMF to obtain FPU. The resultant polymers were precipitated in excess water and dried in a vacuum oven at 60 °C, then redissolved in DMAc and precipitated in an excess methanol/water mixture (1/1, w/w) to remove low molecular weight products. The calculated mass fraction of perfluoroalkyl species to FPU is 31.2%. The purified polymer was washed with methanol and water, and dried in a vacuum oven at 60 °C to get the final FPU. The molecular weight of the final FPU was measured by gel permeation chromatography, and M_w is 33 741 g mol^{-1}. The structural confirmation by ^1H and ^{19}F nuclear magnetic resonance (NMR) spectroscopy and group affirmations by Fourier transform infrared (FT-IR) spectrograph were presented in Figures S2–S4 (Supporting Information).

2.3. Preparation of Polymer Solutions. The FPU/PU solutions were prepared by dissolving FPU and PU in the mixture solvent of DMF/THF (1/1, w/w) with vigorous stirring for 12 h at ambient temperature. The polymers concentrations of the solutions were 1.0, 1.5, 2.5, 3.5, and 4.5 wt %, respectively, and the FPU/PU weight ratio was kept 1:8 in all samples. Additionally, the FPU/PU/CNTs solutions were prepared by dispersing CNTs in the 1.5 wt % FPU/PU solution with ultrasonic treatment for 12 h. The contents of CNTs with respect to the polymers weight were 0.25%, 0.5%, 0.75%, and 1.0%, respectively.

2.4. Solution Properties. Electrical conductivity was measured using a conductivity meter (FE30, Mettler-Toledo Group, Switzerland). Viscosity was tested using a viscometer (SNB-1A, Shanghai Fangrui Instrument Co., Ltd., China) with spindle No. 21 at 50 rpm, and surface tension was determined with tensiometer (QBZY, Shanghai Fangrui Instrument Co., Ltd., China) at ambient temperature.

2.5. Fabrication of the Membranes. The fibrous membranes were fabricated via electrospinning using the DXES-1 spinning equipment (Shanghai Oriental Flying Nanotechnology Co., Ltd., China). Typically, the solution was loaded into a syringe and injected through a metal needle with a controlled feed rate of 5 mL/h. A high voltage of 25 kV was applied to the needle tip, resulting in the generation of a continuous jet stream. The fibrous membranes were deposited on a grounded metallic rotating roller at a 20 cm tip-to-collector distance, and then dried in vacuum oven for 2 h at 80 °C to remove the residual solvent. The electrospinning chamber was kept at a constant temperature (25 °C) and relative humidity (50%). All the membranes were fabricated within an identical thickness of 30 ± 2 μm. The obtained membranes from the FPU/PU solutions were denoted as FPU/PU fibrous membranes, and the ones fabricated from the 1.5 wt % FPU/PU solutions containing different CNTs contents were denoted as FPU/PU/CNTs fibrous membranes. Nonporous membranes with smooth surface were prepared using the dry-casting method. Typically, the polymers solutions were cast uniformly on a glass plate, and were dried in a vacuum oven at 80 °C.

2.6. Characterization of the Membranes. The morphology of the fibrous membranes was observed by field emission scanning electron microscopy (FE-SEM, S-4800, Hitachi Ltd., Japan), all samples were coated with gold for 2 min before analysis. The tensile mechanical property was measured on a tensile tester (XQ-1C, Shanghai New Fiber Instrument Co., Ltd., China) with a crosshead

DOI: 10.1021/acsami.5b02848
ACS Appl. Mater. Interfaces 2015, 7, 13538–13546

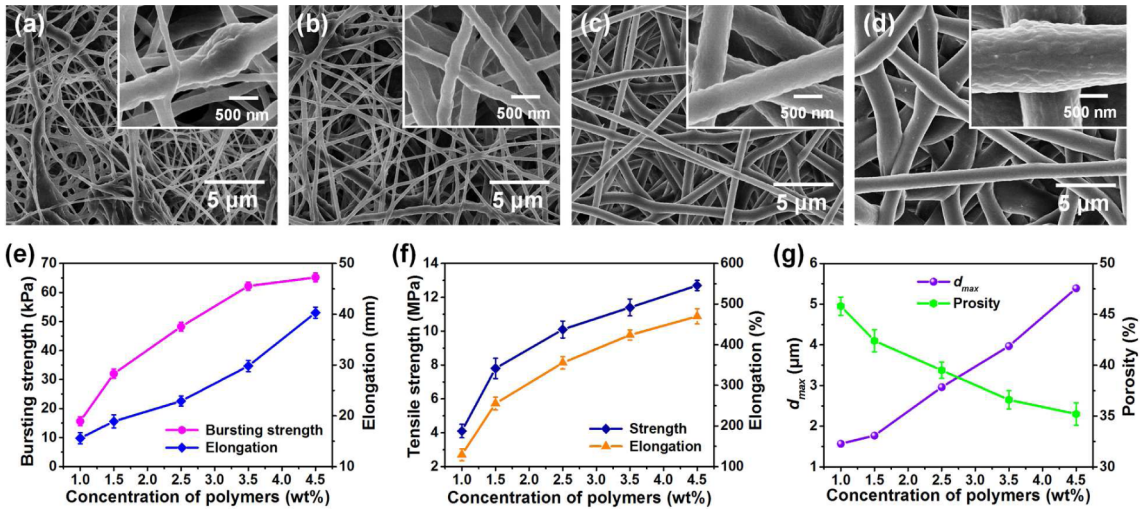

Figure 1. Morphology, mechanical properties, and pore structure of FPU/PU fibrous membranes. FE-SEM images of FPU/PU fibrous membranes fabricated from polymers solutions with different concentrations: (a) 1.0, (b) 1.5, (c) 2.5, and (d) 3.5 wt %, respectively. (e) Bursting strength and elongation, (f) tensile strength and elongation at break, (g) d_{max} and porosity of FPU/PU fibrous membranes fabricated from polymers solutions with different concentrations. The FPU/PU weight ratio was kept 1:8.

speed of 10 mm min^{-1}. The membranes were cut into strips with width of 3 mm as testing samples, and the results were average value of ten samples from each fibrous membrane. The bursting mechanical property was tested on a materials testing machine (H10K-S, Tiniius Olsen Co., Ltd., USA) according to ISO 3303. Circular samples with diameter of 4.5 cm fixed on the machine, and a steel ball was perpendicularly pressed on the membrane with an advancing speed of 300 mm min^{-1}, the results were average value of five samples for each fibrous membrane. Advancing water contact angle (θ_{adv}, 5 μL) of the membranes were measured by a contact angle goniometer Kino SL200B using the increment method. Thickness was measured by a thickness gauge (CHY-C2, Labthink Instruments Co., Ltd., China). The pore size was characterized via bubble point method using a capillary flow porometer (CFP-1100AI, Porous Materials Inc., USA). Porosity of the fibrous membranes were calculated as

$$\text{porosity} = \frac{(D_0 - D_1)}{D_0} \times 100\% \quad (1)$$

where D_0 was the density of the raw PU materials and D_1 was the density of the obtained fibrous membranes.[26]

2.7. Measurements of Waterproof and Breathable Performance. The waterproofness of the membranes were investigated by examining hydrostatic pressure of water penetration, according to AATCC 127 standard test method for water penetration by using a hydrostatic pressure tester (YG812C, Nantong Hongda Experiment Instruments Co., Ltd., China). The samples were covered by a Nylon woven fabric to avoid deformation, and the water pressure increasing rate is 6 kPa/min. The breathable performance was evaluated by measuring the WVT rate according to ASTM E96-$CaCl_2$ standards desiccant method by using a water vapor transmission tester (YG 601H, Ningbo Textile Instruments Co., Ltd., China), under constant temperature of 38 °C and relative humidity of 90%.

3. RESULTS AND DISCUSSION

3.1. FPU/PU Fibrous Membranes. To obtain membranes with waterproof and breathable properties, in the present work we designed hydrophobic fibrous membranes using FPU and PU mixed solutions with different polymers concentrations (1.0−4.5 wt %). The representative FE-SEM images of FPU/PU fibrous membranes obtained by varying the polymers concentrations of FPU/PU solutions are presented in Figures 1 and S5 (Supporting Information), revealing that the fibers oriented randomly to form three-dimensional macroporous structures, which could serve as interconnected passageway for water and vapor. When FPU/PU fibrous membrane was fabricated from 1.0 wt % polymers solution, bead-on-string structures could be clearly observed (as shown in Figure 1a), which constructed with thin fibers (average diameter of 162 nm, Table S1, Supporting Information) and numerous microsized elliptical beads (average diameter of 1.46 μm) along the fiber axis. This structure could be caused by the employment of solutions with low polymers concentration and low viscosity (as shown in Table S1, Supporting Information), which induced the instable whipping of solution jet during electrospinning.[27,28] However, affected by the solutions viscosity, the increase of polymers concentrations from 1.0 to 1.5 wt % led to disappearance of beads and increased fiber diameter (272 nm), as presented in Figure 1b. Further increase of polymers concentration from 2.5 to 4.5 wt % resulted in gradual increase of fiber diameter from 757 to 3124 nm (shown in Figures 1c−d and S5, Supporting Information). Meanwhile, adhesion structures among the adjacent fibers could be observed obviously in all the samples, which could be formed because of the incomplete evaporation of DMF used as good solvent for both FPU and PU.[29,30] The formation of adhesion structure made the electrospun fibers into a dimensionally stable network, which would improve the mechanical properties of the membranes.

Owing to the structure transformation of the fibers and the existence of adhesion structures, mechanical properties of the fibrous membranes would be affected distinctly, which were evaluated by measuring bursting strength normal to the long axis and tensile strength along the long axis of the membranes.[31] As shown in Figure 1e, the FPU/PU fibrous membrane formed from 1.0 wt % polymers solution exhibits the minimum bursting strength (15.6 kPa) and elongation (15.6 mm), which is mainly due to the bead-on-string structures and small fiber diameter that could not afford high external stress.[2,31] However, with the disappearance of beads and the increase of fiber diameter, the membranes fabricated from higher polymers concentrations exhibit enhanced bursting strength up to 65.2 kPa and increased elongation up to 40.3 mm (details are presented in Table S2, Supporting

DOI: 10.1021/acsami.5b02848
ACS Appl. Mater. Interfaces 2015, 7, 13538−13546

Information). Similarly, the minimum tensile strength (4.1 MPa) and elongation (129.1%) was observed at the polymers concentrations of 1.0 wt %, as shown in Figure 1f. Moreover, a sharp increase of tensile mechanical properties could be observed with the polymers concentration increasing to 1.5 wt % according to the transformation of fibers structure, wherein, the tensile strength at break is 7.8 MPa and the elongation is 255.1%. Further increase of polymers concentrations to 4.5 wt % resulted in sizable increased tensile strength up to 12.7 MPa and elongation up to 469.8% (details are presented in Table S2, Supporting Information). These results demonstrate that the mechanical properties could be improved with the increasing of concentrations of polymers solutions, which would attributed to the increase of fiber diameter that provided stronger individual fibers, as well as the existence of adhesion structures that prevented the randomly oriented fibers from pulling apart.[32]

In the meantime, the porous structure of FPU/PU fibrous membranes had been changed remarkably along with the transformation of fibers structure. Since liquid water would preferentially penetrate into a porous media under relative low external pressure through the pore with maximum diameter,[33,34] maximum pore diameters (d_{max}) of the FPU/PU fibrous membranes were measured via bubble point method. As presented in Figure 1g, with the polymers concentrations increased from 1.0 to 4.5 wt %, the d_{max} of the FPU/PU fibrous membranes increased from 1.57 to 5.39 μm (details are shown in Table S3, Supporting Information), which could be attributed to the accumulating of thicker fibers that formed larger space among the adjacent fibers.[35] Additionally, the porosity of the membranes were calculated as well, which would stand for the capacity of interconnected passageway. As shown in Figure 1g, the porosity of FPU/PU fibrous membranes decreased from 45.8% to 35.2% (details are shown in Table S3, Supporting Information)with the of polymers concentrations increasing from 1.0 to 4.5 wt %. These transmission of porosity could be related to the thicker fibers and higher adhesion rate that took over more space among fibers, which is consistent well with the precious studies.[36,37]

More interestingly, it also should be noticed that hierarchical surface structures with micro/nanoscale wrinkles are clearly visible in the close observations of all samples (insets in Figure 1a–d). The formation of these structures would be attributed to the low surface tension and electrical repulsion of solution jet containing FPU as low surface energy content, which generated collapse on the fluid jet surface during fast phase separation, similar to our previous reports.[17,38] It is noteworthy that the cooperation of low surface energy additive and hierarchical surface structure is considered to be strategic factor for surface hydrophobicity, attributing to the entrapped air among the wrinkles like a repulsive cushion to water droplets, as stated previously. As expected, all the FPU/PU fibrous membranes exhibited hydrophobic surface with θ_{adv} reached up to 146 ± 2° (as shown in Table S4, Supporting Information), which would contribute to the resistance to liquid water penetration.[17,39] Furthermore, θ_{adv} of dry-casting membranes were also tested, which could exclude the effect of macro-sized surface morphology of the membranes and represent the surface properties of the inner pores. As shown in Table S4, Supporting Information, the θ_{adv} of the all the dry-casting membranes were 117°, which could be propitious to stimulate the flow process of liquid water in the pores.[40]

Benefiting from hydrophobic properties, FPU/PU fibrous membranes were endowed with waterproofness, which was evaluated by measuring the hydrostatic pressure for water penetration. As presented in Figure 2a, FPU/PU fibrous

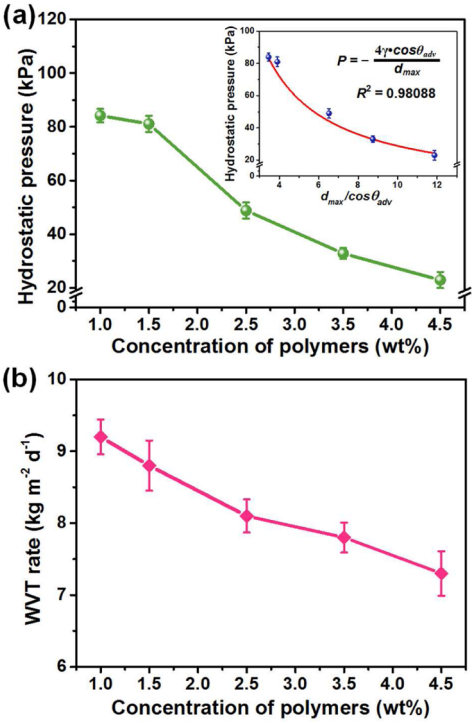

Figure 2. Waterproof and breathable properties of FPU/PU fibrous membranes. (a) Hydrostatic pressure and (b) WVT rate of FPU/PU fibrous membranes fabricated from polymers solutions with various concentrations. The inset in panel a showing the relationship among hydrostatic pressure, d_{max} and θ_{adv}.

membrane obtained from 1.0 wt % polymers solution exhibits the best waterproofness with hydrostatic pressure of 84.2 kPa. Subsequently, with the increase of polymers concentration to 1.5 wt %, the hydrostatic pressure goes down slightly to 81.1 kPa. And further increase of polymers concentrations resulted in dramatically decrease of hydrostatic pressure. Since all the membranes exhibit similar wettability, the decreased hydrostatic pressure of membranes obtained from higher polymers concentrations should be mainly attributed to the enormous increased d_{max}, which would be penetrated under lower external water pressure.[41] Further investigation of the relationship among hydrostatic pressure, hydrophobicity and pore size was carried out by employing the Young–Laplace equation, which is commonly used to express the liquid enter pressure of a cylindrical capillary

$$P = -\frac{4\gamma\cdot\cos\theta_{adv}}{d_{max}} \quad (2)$$

where P is the hydrostatic pressure, γ is the surface tension of water, θ_{adv} is the advancing water contact angle of dry-casting membranes, and d_{max} is the diameter of the maximum pores.[42,43] Significantly, as shown in the inset in Figure 2a, the relationship among hydrostatic pressure, d_{max} and θ_{adv} has been confirmed finely accordance with the Young–Laplace equation.

DOI: 10.1021/acsami.5b02848
ACS Appl. Mater. Interfaces 2015, 7, 13538–13546

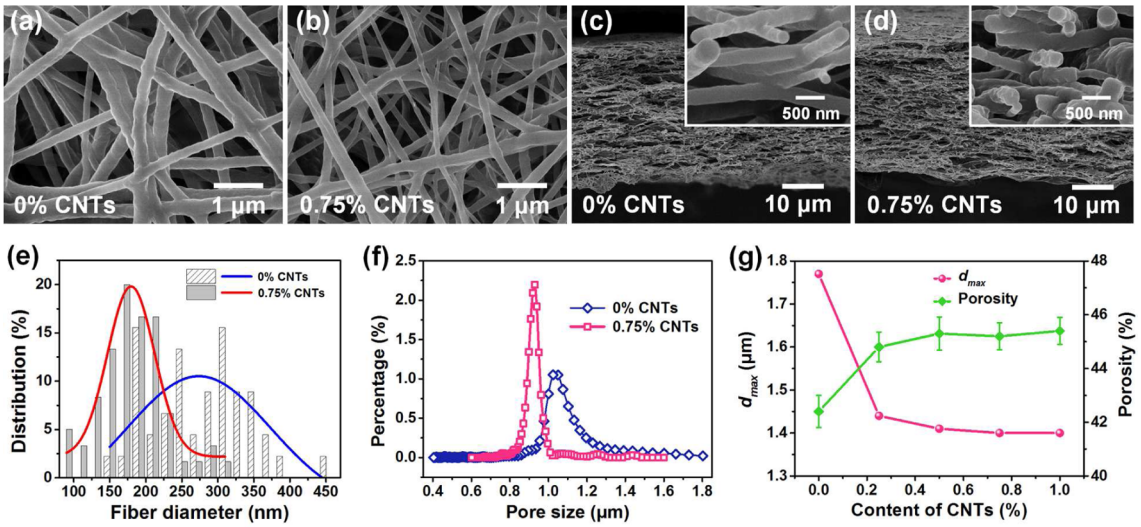

Figure 3. Structure of FPU/PU/CNTs fibrous membranes. FE-SEM images of FPU/PU/CNTs fibrous membranes containing different CNTs contents: (a) 0% and (b) 0.75%. Cross section images of FPU/PU/CNTs fibrous membranes containing different CNTs contents: (c) 0% and (d) 0.75%. (e) Fiber diameter distribution of FPU/PU/CNTs fibrous membranes containing 0% and 0.75% CNTs. (f) Pore size distribution and (g) d_{max} and porosity of FPU/PU/CNTs fibrous membranes containing various contents of CNTs. The FPU/PU concentration of all the solutions was kept 1.5 wt %, and the FPU/PU weight ratio was kept 1:8.

On the other hand, the macroporous structure in FPU/PU fibrous membranes would play a role as interconnected passageway for water vapor transmitting across the membranes, which perform as breathability of membranes. Therefore, WVT rate of FPU/PU fibrous membranes obtained from different polymers concentrations had been measured to estimate the breathability. As shown in Figure 2b, the WVT rate of the fibrous membranes decreased from 9.2 to 7.3 kg m^{-2} d^{-1} gradually with the increase of polymers concentrations, revealing impaired breathability. This would be attributed to that membranes with lower porosity possess less interconnected passageway for water vapor transmission.[36,44] Considering the practical application, the membranes should not only possess good mechanical properties, but also exhibit high waterproof and breathable performance. Since lower polymers concentration (<1.5 wt %) would result in bead-on-string structure and tremendous depression of mechanical properties, as well as higher polymers concentration (>1.5 wt %) could lead to inappropriate porous structure and remarkable reduction of waterproof and breathable performance, the FPU/PU fibrous membranes fabricated from 1.5 wt % polymers solution would be carried out in the following study.

3.2. FPU/PU/CNTs fibrous membranes. To further explore the applicability of the fibrous membranes for waterproof and breathable application, herein, FPU/PU/CNTs fibrous membranes containing various CNTs contents (0−1.0% with respect to polymers weight) were investigated, the polymers concentration of the solutions were kept 1.5 wt %. To study the morphology transformation generated from the addition of CNTs, a comparison between FPU/PU/CNTs fibrous membranes containing 0% and 0.75% CNTs was investigated by FE-SEM images and cross section images, as shown in Figure 3a−d. The FPU/PU/CNTs fibrous membranes without CNTs loading exhibits fiber diameter of 272 nm (as described above) and broad fiber diameter distribution ranging from 140 to 440 nm (as shown in Figure 3e), which could be attributed to the conductivity and viscosity of 1.5 wt % polymers solutions that is appropriate for the disappearance of beads but not adequate for effective stretching of solution jet to provide uniform fibers.[28] However, the FPU/PU/CNTs fibrous membranes containing 0.75% CNTs reveals thinner fiber diameter of 180 nm (Figure 3b) and narrower fiber diameter distribution ranging from 100 to 310 nm (as shown in Figure 3e). This would be related to the increased conductivity that could inspired the stretching effect during electrospinning process, as well as the slightly increased viscosity that could afford more intense whipping.[45,46]

At the meantime, the macroporous structure FPU/PU/CNTs fibrous membranes containing 0% and 0.75% CNTs was investigated by FE-SEM cross section images, revealing that the fibers accumulated layer-by-layer to construct interconnected porous structures, as shown in Figure 3c and d. As can be seen in Figure 3c, the fibrous membranes containing 0% CNTs exhibits irregular porous structure with pore size distribution from 0.40 to 1.77 μm (as shown in Figure 3f), which is related to the accumulation of fibers with ununiformed diameter. However, more regular porous structure with pore size distribution from 0.58 to 1.40 μm (as shown in Figure 3f) would be observed in the membranes containing 0.75% CNTs. It is mainly due to the increased solutions conductivity, which not only generated fibers with uniform diameter, but also brought about densely accumulated fibers.[47,48] Similar transformation also occurred in the other FPU/PU/CNTs fibrous membranes with various CNTs concentrations (as shown in Figure S6, Supporting Information). Accordingly, benefiting from the introduction of CNTs and the transformation of fiber diameter, the d_{max} of FPU/PU/CNTs fibrous membranes decreased from 1.77to 1.40 μm gradually, and the porosity increased slightly from 43.4% to 45.5% (as shown in Figure 5g and Table S3, Supporting Information).

Moreover, with the addition of CNTs, more rough structure had been formed on the surface of fibers (as can be seen in Figure 3d), which is similar to the previous studies and would influence the hydrophobicity of the inner pores.[49] As a result, θ_{adv} of the fibrous membranes and the dry-casting membranes increased to 155° and 122°, respectively, as shown in Table S4 and Figure S7 (Supporting Information), indicating an

DOI: 10.1021/acsami.5b02848
ACS Appl. Mater. Interfaces 2015, 7, 13538−13546

increased hydrophobicity, which would lead to higher resistance to water penetration.

As expected, the optimized porous structure and improved surface hydrophobicity have led to better waterproofness. As shown in Figure 4a, the hydrostatic pressure of FPU/PU/CNTs fibrous membranes with 0.25%, 0.5%, 0.75%, and 1.0% CNTs were 98, 104, 108, and 109 kPa, respectively, which increased regularly with the decreasing of d_{max} and the increasing of θ_{adv}. Furthermore, as can be seen in the inset of Figure 4a, the relationship among hydrostatic pressure, d_{max}, and θ_{adv} is finely conformed to the Young–Laplace equation.[23,24] Meanwhile, with the contents of CNTs increasing from 0% to 1.0%, the WVT rate increased from 8.8 to 9.3 kg m^{-2} d^{-1}, as presented in Figure 4b. This would be attributed to that membranes with higher porosity could provide more interconnected passageway for vapor transmission, which exhibit better breathability. More interestingly, a demonstration of waterproofness and breathable performances has been presented in Figure S8 (Supporting Information), wherein, the FPU/PU/CNTs fibrous membrane was covered on a beaker with boiling water, and three placed water droplets could not penetrate into the membrane while massive vapor transmitted facilely through the membrane. Significantly, the optimized FPU/PU/CNTs fibrous membranes exhibit better comprehensive performance in comparison of the conventional waterproof and breathable materials, as presented in Figure S9 (Supporting Information).

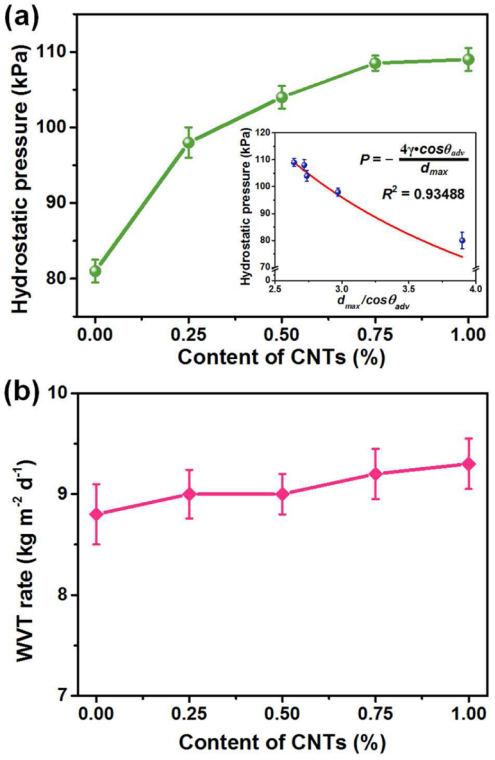

Figure 4. Waterproof and breathable properties of FPU/PU fibrous membranes. (a) Hydrostatic pressure and (b) WVT rate of FPU/PU/CNTs fibrous membranes containing various contents of CNTs. The inset in panel a is the relationship among hydrostatic pressure, d_{max}, and θ_{adv}.

Mechanical properties are important factors in practical application of waterproof and breathable membranes, which would be notably influenced by the loading of CNTs. one of the mechanical properties is bursting strength which would directly characterize the resistance to external pressure perpendicular to the membranes. As shown in Figure 5a, with the CNTs increasing to 0.75%, the bursting strength increased to 47.6 kPa, which would related to the reinforcement of CNTs (details are shown in Table S2, Supporting Information).[46,50] However, further increase of CNTs to 1.0% led to decreased bursting strength of 30.0 kPa. This could mainly due to beads structure formed by the agglomeration of CNTs at higher content (as shown in Figure S10, Supporting Information), which would serve as stress concentrations that break prematurely.[51,52] Meanwhile, the elongation of the membranes decreased gradually with higher loadings of CNTs, indicating

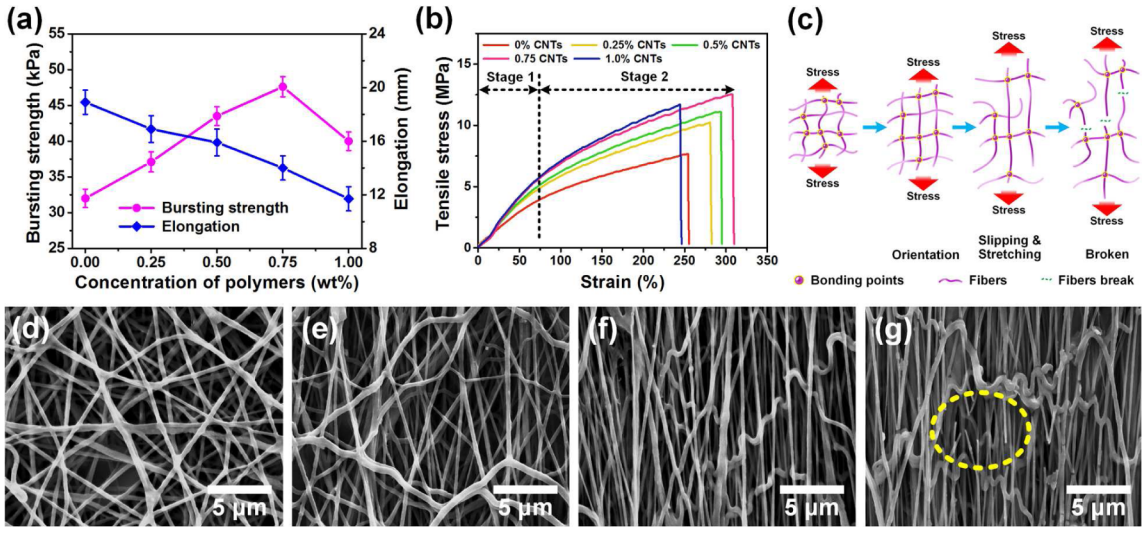

Figure 5. Mechanical properties of FPU/PU/CNTs fibrous membranes. (a) Bursting strength and elongation and (b) tensile stress–strain curves of the FPU/PU/CNTs fibrous membranes containing different contents of CNTs. (c) Proposed break mechanism of tensile fracture process upon external stress. (d–g) In situ SEM images of stretching process of the FPU/PU/CNTs fibrous membranes containing 0.75% CNTs with different elongation: (d) 0%, (e) 50%, (f) 150%, and (g) 300%, respectively.

DOI: 10.1021/acsami.5b02848
ACS Appl. Mater. Interfaces 2015, 7, 13538–13546

that the membranes would exhibit better dimensional stability under external water pressure.

At the same time, tensile strength is another mechanical property which would be significant to the subsequent process of the membranes. Figure 5b presents the typical tensile stress−strain curves of FPU/PU/CNTs fibrous membranes containing various CNTs contents. Similar to the bursting mechanical property, the membranes demonstrated increased tensile strength from 7.8 to 12.5 MPa with the content of CNTs increasing to 0.75%, which revealed the reinforcement effect of CNTs.[46,50] However, owing to the agglomeration of CNTs with content of 1.0%, a reduction of tensile strength to 11.7 MPa could be observed. Moreover, all samples reveal same nonlinear curve shape with little elongation under small stress loading (Stage 1 in Figure 5b) and large elongation under little further increase of stress until broken (Stage 2 in Figure 5b). This phenomenon could be illustrated by the two-step break mechanism (as shown in Figure 5c), which has been demonstrated by in situ FEM images of the stretching process (Figure 5d−g). When a small external stress was loaded, nonaligned fibers (Figure 5d) between bonding points started to orientate (Figure 5e), which led to little elongation. With continual increasing of tensile stress, the nonbonding fibers slipping apart, while the fibers between bonding points undertook the stress and became orientated and thinner (Figure 5f), which resulted in rapid increase of elongation. Finally, the fibrous membranes broke due to the fracture of fibers between bonding points, which was marked with yellow circle (Figure 5g). Consequently, the above waterproof, breathable and mechanical properties suggest the FPU/PU/CNTS fibrous membrane as a promising candidate for a variety of potential applications, such as protective clothing, filter and separator media, and medical supplies.

4. CONCLUSIONS

In summary, we have described the fabrication of FPU/PU/CNTs fibrous membranes exhibiting excellent waterproof and breathable performance. The introduction of FPU and CNTs endowed the resultant membranes with hydrophobic surface properties. Uniform pore structure and decreased maximum pore diameter were obtained with the addition of CNTs. Significantly, the dependence of hydrostatic pressure on d_{max} and θ_{adv} was confirmed to be finely accordance with the Young−Laplace equation. Consequently, the as-prepared membranes containing 0.75% CNTs exhibited excellent waterproofness of 108 kPa, high water vapor transmission rate of 9.2 kg m^{-2} d^{-1}, as well as good mechanical properties with bursting strength of 47.6 kPa and tensile strength of 12.5 MPa. These properties suggest the FPU/PU/CNTS fibrous membrane as a promising candidate for a variety of potential applications, such as protective clothing, filter, and separator media.

■ ASSOCIATED CONTENT

Supporting Information

Schematic diagram illustrating the strategy for synthesis of FPU (Figure S1), ^{1}H NMR spectrum of FPU (Figure S2), ^{19}F NMR spectrum of FPU (Figure S3), FT-IR spectrum of FPU (Figure S4), FE-SEM image of FPU/PU fibrous membrane fabricated from 4.5 wt % polymers solution (Figure S5), compositions and properties of the polymers solutions (Table S1), mechanical properties of the fibrous membranes (Table S2), d_{max} and porosity of the fibrous membranes (Table S3), θ_{adv} of fibrous membranes and dry-casting membranes (Table S4), pore size distribution of FPU/PU/CNTs fibrous membranes containing 0.25%, 0.5%, and 0.75% CNTs (Figure S6), θ_{adv} of the FPU/PU/CNTs dry-casting membranes (Figure S7), a demonstration of waterproof and breathable performance (Figure S8), a comparison of waterproof and breathable properties between current materials and FPU/PU/CNTs fibrous membrane containing 0.75% CNTs (Figure S9), and FE-SEM image of FPU/PU/CNTs fibrous membrane containing 1.0% CNTs (Figure S10). The Supporting Information is available free of charge on the ACS Publications website at DOI: 10.1021/acsami.5b02848.

■ AUTHOR INFORMATION

Corresponding Author

*E-mail: binding@dhu.edu.cn.

Author Contributions

The manuscript was written through contributions of all authors. All authors have given approval to the final version of the manuscript.

Notes

The authors declare no competing financial interest.

■ ACKNOWLEDGMENTS

This work is supported by the National Natural Science Foundation of China (No. 51473030 and 51322304), the Fundamental Research Funds for the Central Universities, and the "DHU Distinguished Young Professor Program".

■ REFERENCES

(1) Lomax, G. R. Breathable Polyurethane Membranes for Textile and Related Industries. *J. Mater. Chem.* **2007**, *17*, 2775.

(2) Wang, X. F.; Ding, B.; Yu, J. Y.; Wang, M. R. Engineering Biomimetic Superhydrophobic Surfaces of Electrospun Nanomaterials. *Nano Today* **2011**, *6*, 510−530.

(3) Gugliuzza, A.; Drioli, E. PVDF and HYFLON AD Membranes: Ideal Interfaces for Contactor Applications. *J. Membr. Sci.* **2007**, *300*, 51−62.

(4) Lalia, B. S.; Guillen-Burrieza, E.; Arafat, H. A.; Hashaikeh, R. Fabrication and Characterization of Polyvinylidenefluoride-co-Hexafluoropropylene (PVDF-HFP) Electrospun Membranes for Direct Contact Membrane Distillation. *J. Membr. Sci.* **2013**, *428*, 104−115.

(5) Gugliuzza, A.; Drioli, E. A Review on Membrane Engineering for Innovation in Wearable Fabrics and Protective Textiles. *J. Membr. Sci.* **2013**, *446*, 350−375.

(6) Rivin, D.; Kendrick, C. E.; Gibson, P. W.; Schneider, N. S. Solubility and Transport Behavior of Water and Alcohols in Nafion. *Polymer* **2001**, *42*, 623−635.

(7) Zhou, C.; Wang, Z.; Liang, Y. L.; Yao, J. M. Study on the Control of Pore Sizes of Membranes Using Chemical Methods Part II. Optimization Factors for Preparation of Membranes. *Desalination* **2008**, *225*, 123−138.

(8) Gugliuzza, A.; Drioli, E. New Performance of Hydrophobic Fluorinated Porous Membranes Exhibiting Particulate-Like Morphology. *Desalination* **2009**, *240*, 14−20.

(9) Tabatabaei, S. H.; Carreau, P. J.; Ajji, A. Microporous Membranes Obtained from Polypropylene Blend Films by Stretching. *J. Membr. Sci.* **2008**, *325*, 772−782.

(10) Pan, J. H.; Dou, H.; Xiong, Z.; Xu, C.; Ma, J.; Zhao, X. S. Porous Photocatalysts for Advanced Water Purifications. *J. Mater. Chem.* **2010**, *20*, 4512−4528.

(11) Yu, B.; Han, J.; He, X. B.; Xu, G. P.; Ding, X. B. Effects of Tourmaline Particles on Structure and Properties of Polypropylene Filtration Melt-Blown Nonwoven Electrets. *J. Macromol. Sci., Part B: Phys.* **2012**, *51*, 619−629.

DOI: 10.1021/acsami.5b02848
ACS Appl. Mater. Interfaces 2015, 7, 13538−13546

(12) Wang, X. F.; Ding, B.; Sun, G.; Wang, M. R.; Yu, J. Y. Electro-Spinning/Netting: A Strategy for the Fabrication of Three-Dimensional Polymer Nano-Fiber/Nets. *Prog. Mater. Sci.* **2013**, *58*, 1173−1243.
(13) Erisken, C.; Kalyon, D. M.; Wang, H. J. Functionally Graded Electrospun Polycaprolactone and Beta-Tricalcium Phosphate Nanocomposites for Tissue Engineering Applications. *Biomaterials* **2008**, *29*, 4065−4073.
(14) Wang, X. F.; Ding, B.; Li, B. Y. Biomimetic Electrospun Nanofibrous Structures for Tissue Engineering. *Mater. Today* **2013**, *16*, 229−241.
(15) Park, C. H.; Chung, S. E.; Yun, C. S. Effect of Drying Condition on the Electrostatic Characteristics of the Laundry. *Fibers Polym.* **2007**, *8*, 432−437.
(16) Yoon, B.; Lee, S. Designing Waterproof Breathable Materials Based on Electrospun Nanofibers and Assessing the Performance Characteristics. *Fibers Polym.* **2011**, *12*, 57−64.
(17) Ge, J. F.; Si, Y.; Fu, F.; Wang, J. L.; Yang, J. M.; Cui, L. X.; Ding, B.; Yu, J. Y.; Sun, G. Amphiphobic Fluorinated Polyurethane Composite Microfibrous Membranes with Robust Waterproof and Breathable Performances. *RSC Adv.* **2013**, *3*, 2248−2255.
(18) Wang, J. Q.; Li, Y.; Tian, H. Y.; Sheng, J. L.; Yu, J. Y.; Ding, B. Waterproof and Breathable Membranes of Waterborne Fluorinated Polyurethane Modified Electrospun Polyacrylonitrile Fibers. *RSC Adv.* **2014**, *4*, 61068−61076.
(19) Ko, F.; Gogotsi, Y.; Ali, A.; Naguib, N.; Ye, H.; Yang, G. L.; Li, C.; Willis, P. Electrospinning of Continuous Carbon Nanotube-Filled Nanofiber Yarns. *Adv. Mater.* **2003**, *15*, 1161−1165.
(20) Coleman, J. N.; Khan, U.; Blau, W. J.; Gun'ko, Y. K. Small but Strong: A Review of the Mechanical Properties of Carbon Nanotube-Polymer Composites. *Carbon* **2006**, *44*, 1624−1652.
(21) Kim, B. S.; Harriott, P. Critical Entry Pressure for Liquids in Hydrophobic Membranes. *J. Colloid Interface Sci.* **1987**, *115*, 1−8.
(22) Shirtcliffe, N. J.; McHale, G.; Newton, M. I.; Zhang, Y. Superhydrophobic Copper Tubes with Possible Flow Enhancement and Drag Reduction. *ACS Appl. Mater. Interfaces* **2009**, *1*, 1316−1323.
(23) Bui, N. N.; Lind, M. L.; Hoek, E. M. V.; McCutcheon, J. R. Electrospun Nanofiber Supported Thin Film Composite Membranes for Engineered Osmosis. *J. Membr. Sci.* **2011**, *385*−*386*, 10−19.
(24) Zhou, W. P.; Wu, Y. L.; Wei, F.; Luo, G. H.; Qian, W. Z. Elastic Deformation of Multiwalled Carbon Nanotubes in Electrospun MWCNTs-PEO and MWCNTs-PVA Nanofibers. *Polymer* **2005**, *46*, 12689−12695.
(25) Wang, J. L.; Raza, A.; Si, Y.; Cui, L. X.; Ge, J. F.; Ding, B.; Yu, J. Y. Synthesis of Superamphiphobic Breathable Membranes Utilizing SiO_2 Nanoparticles Decorated Fluorinated Polyurethane Nanofibers. *Nanoscale* **2012**, *4*, 7549−7556.
(26) Mika, A. M.; Childs, R. F.; Dickson, J. M.; McCarry, B. E.; Gagnon, D. R. A New Class of Polyelectrolyte-Filled Microfiltration Membranes with Environmentally Controlled Porosity. *J. Membr. Sci.* **1995**, *108*, 37−56.
(27) Lin, J.; Ding, B.; Yu, J. Direct Fabrication of Highly Nanoporous Polystyrene Fibers via Electrospinning. *ACS Appl. Mater. Interfaces* **2010**, *2*, 521−528.
(28) Greiner, A.; Wendorff, J. H. Electrospinning: A Fascinating Method for the Preparation of Ultrathin Fibers. *Angew. Chem., Int. Ed.* **2007**, *46*, 5670−5703.
(29) Khil, M. S.; Cha, D. I.; Kim, H. Y.; Kim, I. S.; Bhattarai, N. Electrospun Nanofibrous Polyurethane Membrane as Wound Dressing. *J. Biomed. Mater. Res., Part B* **2003**, *67B*, 675−679.
(30) Mao, X.; Chen, Y. C.; Si, Y.; Li, Y.; Wan, H. G.; Yu, J. Y.; Sun, G.; Ding, B. Novel Fluorinated Polyurethane Decorated Electrospun Silica Nanofibrous Membranes Exhibiting Robust Waterproof and Breathable Performances. *RSC Adv.* **2013**, *3*, 7562−7569.
(31) Yao, C.; Li, X. S.; Neoh, K. G.; Shi, Z. L.; Kang, E. T. Surface Modification and Antibacterial Activity of Electrospun Polyurethane Fibrous Membranes with Quaternary Ammonium Moieties. *J. Membr. Sci.* **2008**, *320*, 259−267.
(32) Lee, K. H.; Kim, H. Y.; Ryu, Y. J.; Kim, K. W.; Choi, S. W. Mechanical Behavior of Electrospun Fiber Mats of Poly(vinyl chloride)/Polyurethane Polyblends. *J. Polym. Sci., Part B: Polym. Phys.* **2003**, *41*, 1256−1262.
(33) Hopkinson, D.; Zeh, M.; Luebke, D. The Bubble Point of Supported Ionic Liquid Membranes Using Flat Sheet Supports. *J. Membr. Sci.* **2014**, *468*, 155−162.
(34) Wang, R.; Liu, Y.; Li, B.; Hsiao, B. S.; Chu, B. Electrospun Nanofibrous Membranes for High Flux Microfiltration. *J. Membr. Sci.* **2012**, *392*−*393*, 167−174.
(35) Li, X.; Wang, N.; Fan, G.; Yu, J. Y.; Gao, J.; Sun, G.; Ding, B. Electreted Polyetherimide-Silica Fibrous Membranes for Enhanced Filtration of Fine Particles. *J. Colloid Interface Sci.* **2015**, *439*, 12−20.
(36) Ryu, Y. J.; Kim, H. Y.; Lee, K. H.; Park, H. C.; Lee, D. R. Transport Properties of Electrospun Nylon 6 Nonwoven Mats. *Eur. Polym. J.* **2003**, *39*, 1883−1889.
(37) Gibson, P.; Schreuder-Gibson, H.; Rivin, D. Transport Properties of Porous Membranes Based on Electrospun Nanofibers. *Colloids Surf., A* **2001**, *187*−*188*, 469−481.
(38) Reneker, D. H.; Yarin, A. L. Electrospinning Jets and Polymer Nanofibers. *Polymer* **2008**, *49*, 2387−2425.
(39) Manabe, K.; Nishizawa, S.; Kyung, K. H.; Shiratori, S. Optical Phenomena and Antifrosting Property on Biomimetics Slippery Fluid-Infused Antireflective Films via Layer-by-Layer Comparison with Superhydrophobic and Antireflective Films. *ACS Appl. Mater. Interfaces* **2014**, *6*, 13985−13993.
(40) Si, Y.; Fu, Q. X.; Wang, X. Q.; Zhu, J.; Yu, J. Y.; Sun, G.; Ding, B. Superelastic and Superhydrophobic Nanofiber-Assembled Cellular Aerogels for Effective Separation of Oil/Water Emulsions. *ACS Nano* **2015**, *9*, 3791−3799.
(41) Manabe, K.; Nishizawa, S.; Shiratori, S. Porous Surface Structure Fabricated by Breath Figures that Suppresses *Pseudomonas aeruginosa* Biofilm Formation. *ACS Appl. Mater. Interfaces* **2013**, *5*, 11900−11905.
(42) Saffarini, R. B.; Mansoor, B.; Thomas, R.; Arafat, H. A. Effect of Temperature-Dependent Microstructure Evolution on Pore Wetting in PTFE Membranes Under Membrane Distillation Conditions. *J. Membr. Sci.* **2013**, *429*, 282−294.
(43) Hu, H.; Larson, R. G. Evaporation of a Sessile Droplet on a Substrate. *J. Phys. Chem. B* **2002**, *106*, 1334−1344.
(44) Yuan, D.; Cheng, H.; Edwards, R. L.; Dykoski, C. A.; Kelly, M. J.; Zhang, M.; Qing, J.; Lin, Y.; Wang, Y.; Wu, J.; Dorale, J. A.; An, Z.; Cai, Y. Timing, Duration, and Transitions of the Last Interglacial Asian Monsoon. *Science* **2004**, *304*, 575−578.
(45) Xie, X. L.; Mai, Y. W.; Zhou, X. P. Dispersion and Alignment of Carbon Nanotubes in Polymer Matrix: A Review. *Mater. Sci. Eng., R* **2005**, *49*, 89−112.
(46) Wang, X.; Si, Y.; Wang, X.; Yang, J.; Ding, B.; Chen, L.; Hu, Z.; Yu, J. Tuning Hierarchically Aligned Structures for High-Strength PMIA-MWCNT Hybrid Nanofibers. *Nanoscale* **2013**, *5*, 886−889.
(47) Zhu, Q.; Li, Y. Effects of Pore Size Distribution and Fiber Diameter on the Coupled Heat and Liquid Moisture Transfer in Porous Textiles. *Int. J. Heat Mass Transfer* **2003**, *46*, 5099−5111.
(48) Lowery, J. L.; Datta, N.; Rutledge, G. C. Effect of Fiber Diameter, Pore Size and Seeding Method on Growth of Human Dermal Fibroblasts in Electrospun Poly(ε-Caprolactone) Fibrous Mats. *Biomaterials* **2010**, *31*, 491−504.
(49) Mathew, G.; Hong, J. P.; Rhee, J. M.; Lee, H. S.; Nah, C. Preparation and Characterization of Properties of Electrospun Poly(Butylene Terephthalate) Nanofibers Filled with Carbon Nanotubes. *Polym. Test.* **2005**, *24*, 712−717.
(50) Dror, Y.; Salalha, W.; Khalfin, R. L.; Cohen, Y.; Yarin, A. L.; Zussman, E. Carbon Nanotubes Embedded in Oriented Polymer Nanofibers by Electrospinning. *Langmuir* **2003**, *19*, 7012−7020.
(51) Su, Z. Q.; Li, J. F.; Li, Q.; Ni, T. Y.; Wei, G. Chain Conformation, Crystallization Behavior, Electrical and Mechanical Properties of Electrospun Polymer−Carbon Nanotube Hybrid Nanofibers with Different Orientations. *Carbon* **2012**, *50*, 5605−5617.

DOI: 10.1021/acsami.5b02848
ACS Appl. Mater. Interfaces 2015, 7, 13538−13546

(52) Coleman, J. N.; Khan, U.; Gun'ko, Y. K. Mechanical Reinforcement of Polymers Using Carbon Nanotubes. *Adv. Mater.* **2006**, *18*, 689−706.

DOI: 10.1021/acsami.5b02848
ACS Appl. Mater. Interfaces 2015, 7, 13538−13546